GSICS Global Space-based Inter-Calibration System

Quarterly

Newsletter– Winter 2019 Issue

CMA • CNES • ESA • EUMETSAT • IMD • ISRO • JAXA • JMA • KMA • NASA • NIST • NOAA • ROSCOSMOS . ROSHYDROMET • SITP • USGS • WMO

In this Issue

Integration of observing systems within the WIGOS framework. (Image Curtesy WMO)

Image above shows the location of GOES-17, which recently became operational as GOES-WEST

The Quest for Consistency in Remote Sensing

By Xavier Calbet, AEMET, Spain

In the field of satellite remote sensing, it is common practice to combine measurements from different instruments to either generate a satellite product or to be fed into an assimilation system of a Numerical Weather Prediction (NWP) model.

In both cases, the ultimate purpose is to estimate the quantity of diverse atmospheric parameters, either directly as a satellite product or indirectly in an assimilation system. There are several reasons behind this strategy: availability of numerous different instruments, good technical characterization of the instruments and adequate performance of the radiative transfer models.

Inconsistencies
Although instruments are very precise and RTMs have achieved a high degree of accuracy, there is often, in practice, a systematic mismatch between what is observed and what is calculated from the RTMs. Their cause is varied and can range from an incorrect or incomplete implementation of the radiative transfer model setup, to uncalibrated instrumental effects or deviations in their nominal performance.

The Quest for Consistency

Operational systems need to be online 24 hours a day and 7 days a week.

These systems, such as global NWP models, need to find a practical solution to the mismatch between observations. This solution is usually based on a more or less sophisticated form of bias correction for RTMs (e.g. McNally, 2005). From a strictly logical point of view, the ideal situation would be to have them being consistent before using them operationally. But, verifying consistency between measurements is not an easy task, it is an endeavour that can take many resources and much time. Below are a few examples of some of the quests for consistency

GRUAN Radiosondes and IASI Hyperspectral Infrared Consistency
The GCOS Radiosonde Upper Air Network (GRUAN) has made a
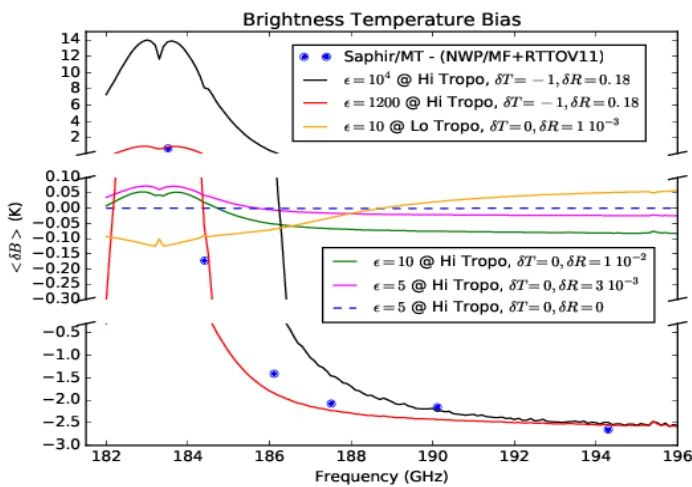
Figure 1. Brightness temperature deviations calculated for different levels in the troposphere, various turbulence intensities, ε in cm² s⁻³, and adjusted offsets in temperature and humidity (R=e/e). Blue dots are values of observed minus calculated brightness temperatures between the SAPHIR Megha-Tropiques instrument vs. Météo France NWP profiles plus the RTTOV v11 RTM (from Brogniez et al., 2016).
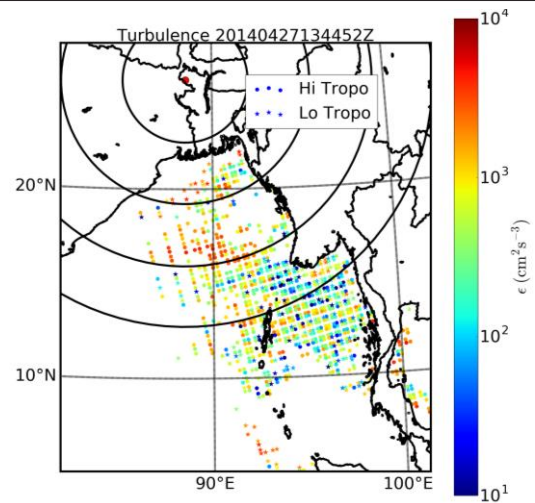
Figure 2. Turbulence intensity (mean energy dissipation rate per unit mass, ε) as derived from the discrepancies between the infrared hyperspectral measurement from IASI and microwave measurements from MHS. Concentric circles are plotted around a Kalboishakhi storm (red dot) following gravity waves in the stratosphere as seen by IASI.

laudable effort into removing biases from radiosonde measurements and determining their uncertainties (Dirksen et al., 2014). The now well-known dry biases from RS92 sonde types (Vömel et al., 2007) are corrected for in the GRUAN radiosonde data processing. This biases can be quite high in some circumstances of high solar illumination. They have also characterized in high detail the uncertainties in the radiosonde measurements. These are the necessary first steps before evaluating any inconsistencies with other measurements (Immler et al. 2010). This background work has made the comparison of measurements from GRUAN sondes with hyperspectral infrared instruments, such as IASI, possible. The comparisons have been made in radiance space, rather than in atmospheric parameter space (temperature or water vapour concentration). This makes the comparisons simpler because all the issues coming from retrievals such as Optimal Estimation (Rodgers, 2000) or

NWP assimilation are avoided. GRUAN sondes and IASI radiances are in good agreement when comparing nighttime radiosonde measurements (Calbet et al. 2017). On the other hand, the daytime radiosonde measurements show an overall remaining dry bias, which is corrected for when adding 2.5% in absolute terms of relative humidity to the complete GRUAN sonde profile.

Microwave and Infrared Sounder Consistency

Microwave measurements show a systematic and relatively large bias when compared with other atmospheric measurements or NWP analyses (Brogniez et al. 2016). It has recently been hypothesized that these discrepancies can come from relatively large variations in water vapor concentration in the atmosphere. This has been shown by Bobryshev et al. (2018), where they select cases where there is a small spatial microwave radiance variation, managing to reduce the initial microwave radiation biases significantly. Taking it a step further,

Calbet et al. (2018) have estimated the effect in the microwave radiances of a large water vapor concentration variability within the field of view of the instrument, which again leads to large microwave radiance biases. This variability is quite common in the atmosphere coming from its inherent turbulent nature. When doing this, the observed biases can be reproduced (Fig. 1). Numerically, the biases come from large second order derivatives in the radiative transfer model together with a big spatial variability in the water vapor field.

In parallel studies, we have seen that the second order derivatives seem to be much smaller in some channels in the infrared, having turbulence intensities yield little impact in these radiances. Therefore, the logical next step is to compare microwave and infrared radiances and check for discrepancies. These discrepancies, if the underlying variability theory is correct, would point out to places where turbulence is

high. A quick test has been done over a region where a severe storm was present over Bangladesh (Mills and Higgins, 2014) on April 27, 2014. This storm caused strong gravity waves in the troposphere and it would logically be expected that it also created strong turbulence in the troposphere. Results are shown in Fig. 2.

Summary

Searching for consistency among different atmospheric measuring instruments is the logical first step before combining these measurements into one product. This task is by no means easy, but it is working in the discrepancies that makes this branch of physics interesting. GSICS, GRUAN and many other groups are now working to achieve this goal. The quest for consistency will remain alive within these groups. We do not know exactly where this quest will lead us. Solutions could range from trivial findings to uncharted territory by means of completely unexpected phenomena. We certainly live in interesting times, where the quest for consistency continues.

References

Bobryshev, O., et. al.: Is There Really a Closure Gap Between 183.31-GHz Satellite Passive Microwave and In Situ Radiosonde Water Vapor Measurements?, TGRS 56, 2904–2910, doi:10.1109/TGRS.2017.2786548, 2018.

Brogniez, H., et al.: A review of sources of systematic errors and uncertainties in observations and simulations at 183 GHz, Atmos. Meas. Tech., 9, 2207-2221,doi: 10.5194/amt-9-2207-2016, 2016.

Calbet, X. and Schlüssel, P.: Technical note: analytical estimation of the optimal parameters for the EOF retrievals of the IASI Level 2 Product Processing Facility and its application using AIRS and ECMWF data, Atmos. Chem. Phys., 6, 831-846, doi: 10.5194/acp-6-831-2006, 2006.

Calbet, X., et al.: Consistency between GRUAN sondes, LBLRTM and IASI, Atmos. Meas. Tech., 10, 2323-2335, doi:10.5194/amt-10-2323-2017, 2017.

Calbet, X., et al.: Can turbulence within the field of view cause significant biases in radiative transfer modeling at the 183 GHz band?, Atmos. Meas. Tech., 11, 6409-6417,doi: 10.5194/amt-11-6409-2018, 2018.

Dirksen, R. J. et. al.: Reference quality upper-air measurements: GRUAN data processing for the Vaisala RS92 radiosonde, Atmos. Meas. Tech., 7, 4463-4490,doi: 10.5194/amt-7-4463-2014, 2014.

Immler, F. J. et. Al : Reference Quality Upper-Air Measurements: guidance for developing GRUAN data products, Atmos. Meas. Tech., 3, 1217–1231, doi:10.5194/amt-3-1217-2010, 2010.

Mills, I., Higgins, M.: A Kalboishakhi storm swept across northern Bangladesh on the evening of 27 April, link

McNally, T.: Introduction to bias estimation and correction for satellite data assimilation, ECMWF/NWP-SAF Workshop on Bias estimation and correction in data assimilation, Reading, 8-11 November 2005.

Rodgers, C. D.: Inverse methods for atmospheric sounding. Theory and practice, World Scientific, Singapore, 2000.

Vömel, H., et al.: Radiation Dry Bias of the Vaisala RS92 Humidity Sensor, J.Atmos. Oceanic Technol., 24, 953–963, 2007.

Discuss the Article

Characterization of Numerical Weather Prediction model Biases and uncertainties for Improved Satellite Cal/Val

By Fabien Carminati (UKMO), Stefano Migliorini (UKMO), and Bruce Ingleby (ECMWF)

Numerical weather prediction (NWP) models have been shown to be suitable reference comparators and are increasingly used for the assessment of satellite instruments (Saunders et al., 2013). Improvements in data assimilation techniques and the ingestion of a large number of observations continuously drive down errors and uncertainties in NWP analyses and short-range forecasts (Bauer et al., 2015) to such an extent that state-of-the-art NWP models can detect biases as small as 0.1 K in satellite observation datasets (Loew et al., 2017). Yet model uncertainty estimates do not meet the international metrological traceability standards recommended by the World Meteorological Organisation (WMO) and Global Space-based Inter-Calibration System (GSICS).

The NWP model error and uncertainty budget can be expressed as a function of four main contributions related to: a) NWP temperature and humidity fields mapped to observation space; b) underlying radiative transfer modelling; c) scale mismatch; and d) undetected cloud. In a recent work, Carminati et al. (2019) proposed a methodology to address the first of these contributions. The authors developed a software,

referred to as the GCOS (Global Climate Observing System) Reference Upper-Air Network (GRUAN) processor, that collocates NWP model fields to GRUAN radiosonde profiles (Dirksen et al., 2014) in space and time, simulates top-of-atmosphere brightness temperatures (T_b) at frequencies used by satellite instruments, and propagates GRUAN uncertainties in radiance space. The GRUAN processor specifics, including interpolations schemes, radiative transfer calculations, and uncertainty propagation, are described by Carminati et al. (2019). Note that the authors advise against the use of satellite channels that are predominantly sensitive to the surface or to the upper atmosphere because GRUAN data products do not provide information at those levels and the resulting simulation become dependent of the collocated model fields.

The propagation of GRUAN uncertainties in T_b space is performed via the perturbation of GRUAN temperature, humidity and pressure profiles by their profiles of total uncertainty assuming that the uncertainty is fully correlated throughout the profile (i.e., if the uncertainty value is added or removed at a given level, it will also be added or removed at all other levels). The authors stress that this is a pessimistic assumption, since the total uncertainty is only partially correlated in the vertical, which results in an overestimation of the uncertainty in T_b space. A better propagation of errors could be achieved by partitioning GRUAN uncertainty into correlated, random, and pseudo random uncertainties, ideally expressed as a full covariance matrix. Furthermore, this approach only accounts for the uncertainty in GRUAN profiles and ignores uncertainties in the NWP model fields and data processing.

<u>Return to Page One</u>

To cope with this caveat, Carminati et al. (2019) additionally proposed a rigorous mathematical methodology to estimate the uncertainty related to the difference NWP minus GRUAN ($\delta \mathbf{y}$) in T_b space based on the processor outputs.

The covariance of GRUAN measurements ($\mathbf{S}_{GRUAN}$), of the NWP fields ($\mathbf{S}_{NWP}$), and of the interpolation carried out by the processor ($\mathbf{S}_{int}$) are calculated in T_b space multiplying the uncertainty by the Jacobians ($\mathbf{H}$) derived from the simulation such as:

$$\mathbf{S}_{GRUAN} = \mathbf{HRH}^T \qquad \ldots\ldots\ldots\ldots(1)$$

$$\mathbf{S}_{NWP} = \mathbf{HWBW}^T\mathbf{H}^T \qquad \ldots\ldots\ldots\ldots(2)$$

$$\mathbf{S}_{int} = \mathbf{HS}^{int}\mathbf{H}^T \qquad \ldots\ldots\ldots\ldots(3)$$

where $\mathbf{R}$ is a diagonal matrix accounting for the different sources of GRUAN uncertainty, $\mathbf{B}$ represents the uncertainties in the NWP fields, $\mathbf{W}$ is the interpolation matrix, and $\mathbf{S}^{int}$ can be shown to be function of $\mathbf{B}$ and $\mathbf{W}$.

The covariance $\mathbf{S}_{\delta \mathbf{y}}$ of the difference $\delta \mathbf{y}$ is calculated as the sum of the GRUAN, NWP fields, and interpolation covariances such as:

$$\mathbf{S}_{\delta \mathbf{y}} \cong \mathbf{S}_{GRUAN} + \mathbf{S}_{NWP} + \mathbf{S}_{int} \ldots\ldots\ldots\ldots(4)$$

The total uncertainty associated with $\delta \mathbf{y}$ is given by the square root of the diagonal of $\mathbf{S}_{\delta \mathbf{y}}$. Note however that the propagation of GRUAN uncertainty in T_b space, and by extension the estimation of $\mathbf{S}_{\delta \mathbf{y}}$, remains suboptimal due to the lack of full GRUAN

covariance matrix estimate. This stresses the need for the GRUAN community to provide error covariance matrices with realistic vertical correlation structures.

For the purposes of demonstration of capability, Carminati et al. (2019) processed and analysed one year of GRUAN radiosonde profiles from Lindenberg, Germany, in 2016, and matching NWP fields from the Met Office and European Centre for Medium-range Weather Forecasts (ECMWF) global models. Focusing on the night-time profiles, Table 1 reports the difference $\delta \mathbf{y}_{MetOffice}$ between T_b simulated from Met Office NWP fields and those from GRUAN profiles and associated uncertainty for the frequencies used by the Advanced Technology Microwave Sounder (ATMS). At frequencies predominantly sensitive to temperature (54-57 GHz) the difference lies from -0.09 to 0.04 K with uncertainties ranging from 0.08 to 0.13 K. At frequencies predominantly sensitive to humidity (183 GHz) the difference lies between -0.46 and 0.02 K with uncertainties ranging from 1.66 to 2.59 K. Assessed with a χ^2 test, the authors reported that 90 % of the comparisons were found to be in statistical agreement.

Future studies will focus on the analysis of collocated profiles spanning several years and multiple GRUAN sites and will contribute to achieve a better (although still incomplete) understanding of the geographical

Table 1: Mean $\delta \mathbf{y}_{MetOffice}$, 1$\sigma$ standard deviation, and associated uncertainty of 587 Lindenberg night-time profiles simulated for ATMS channels 8-12 and 18-22.

Channel	Frequency (GHz)	$\delta \mathbf{y}_{MetOffice}$ (1σ) (K)	Uncertainty (K)
8	54.94	-0.00 (0.11)	0.08
9	55.5	0.04 (0.13)	0.08
10	57.29	0.01 (0.16)	0.12
11	57.29±0.217	-0.04 (0.20)	0.12
12	57.29±0.3222±0.048	-0.09 (0.28)	0.13
18	183.31±7.0	0.02 (0.83)	1.66
19	183.31±7.0	-0.09 (1.03)	1.71
20	183.31±3.0	-0.18 (1.22)	1.99
21	183.31±1.8	-0.31 (1.42)	2.34
22	183.31±1.0	-0.46 (1.57)	2.59

distribution of model uncertainties for key frequencies selected both in the microwave and infrared domains. This work also aims to establish a methodology to determine the full model uncertainty budget which can be used for a more robust assessment of satellite observations. Additionally, processor-based studies are expected to provide beneficial applications for data assimilation systems such as an improved estimate of the NWP model's forecast error covariance matrices or the observation bias corrections used in NWP centres.

References:

Bauer, P., et al.: The quiet revolution of numerical weather prediction, Nature, 525, 47, doi: 10.1038/nature14956, 2015.

Carminati, F., et al.: Using reference radiosondes to characterise NWP model uncertainty for improved satellite calibration and validation, Atmos. Meas. Tech., 12, 83-106, doi: 10.5194/amt-12-83-2019, 2019.

Dirksen, R. J., et al.: Reference quality upper-air measurements: GRUAN data processing for the Vaisala RS92 radiosonde, Atmos. Meas. Tech., 7, 4463-4490,doi: 10.5194/amt-7-4463-2014, 2014.

Loew, A., et al.: Validation practices for satellite based earth observation data across communities, Reviews of Geophysics, 55, 779–817, doi:10.1002/2017RG000562, 2017.

Saunders, R. W., et al.: Monitoring satellite radiance biases using NWP models, IEEE Trans. Geosci. Remote Sens., 51(3), 1124–1138, doi: 10.1109/TGRS.2012.2229283

In-Orbit Calibration of Second-generation Global Imager (SGLI) onboard GCOM-C "SHIKISAI"

By Yoshihiko Okamura, Shigemasa Ando, Tomoyuki Urabe and Kazuhiro Tanaka (JAXA)

The Japan Aerospace Exploration Agency (JAXA) is pressing forward with the Global Change Observation Mission (GCOM) for long-term monitoring of the Earth's environment to facilitate understanding the global water circulation and climate change, and eventually contribute to improving future climate projections through a collaborative framework with climate model institutions [1]. GCOM consists of two polar orbiting satellite observing systems, GCOM-W "SHIZUKU" and GCOM-C "SHIKISAI". GCOM-W with Advance Microwave Radiometer - 2 (AMSR-2) and GCOM-C with Second-generation Global Imager (SGLI) were launched in 2012 and 2017, respectively, and have been observing the Earth continuously.

SGLI is an optical multi-band imaging radiometer in the wavelength range of near-UV to thermal infrared [2]. It consists of two sensor units, Visible and Near Infrared Radiometer (SGLI-VNR) and Infrared Scanning Radiometer (SGLI-IRS). SGLI performs multi-band (380nm-12µm) optical observation not only with a wide FOV (field of view) of 1150-1400 km but also a relatively high resolution of 250 m. In addition, polarization and along-track slant view observation are one of the unique features of SGLI.

On-board calibration of VNR bands is achieved by solar light and internal lamps reflected by a Spectralon® diffuser. VNR is equipped with a deployable diffuser to illuminate the uniformly scattered sunlight to VNR telescopes. White and near-infrared LEDs are also used for internal light calibration.

IRS employs a continuously rotating scanning mirror to allow us to conduct the on-board calibration every scan; a high emissivity blackbody calibrator for TIR bands and a deep space port for all the IRS bands. In addition, the Spectralon® solar diffuser and LED/Halogen lamp assembly is utilized for the SWIR radiometric calibration.

The calibration data obtained by the onboard calibrators allow us to perform in-orbit radiometric evaluation such as gain, signal-to-noise ratio (SNR), dynamic range, linearity, and relative band-to-band spectral response.

In-orbit SGLI calibration methodologies and operations are summarized in Figure 2 [3] [4]. On-board calibration of reflective solar bands (VNR and IRS-SWIR bands) is achieved by weekly solar and internal lamp calibrations.

Regarding the thermal emissive band (IRS-TIR bands), the continuously rotating scanning mirror allows to conduct the on-board calibration every scan using the blackbody calibrator and the deep space port.

In addition to these calibration methods using the onboard calibrators, GCOM-C has three kinds of dedicated maneuver operation; i) lunar calibration pitch maneuver, ii) solar angle correction yaw maneuver and iii) 90-deg. yaw maneuver for pixel-to-pixel non-uniformities. As for the SGLI lunar calibration pitch maneuver, the lunar observation images captured by maneuvering GCOM-C attitude around the pitch axis are used as radiometric calibration data for the reflective solar bands. The moon reflects solar light and is a stable light source suitable as a long-term calibration light source. Throughout the entire GCOM-C operation periods, the lunar calibration operation will be performed approximately every 29 days when the lunar phase angle is around 7°. The lunar calibration data is evaluated using the GSICS lunar calibration tool (GIRO: GSICS Implementation of the Robotic Lunar Observatory).

As a result of the initial in-orbit calibration activities, all the SGLI functions are operating properly and SGLI maintains the predicted

GCOM-C SGLI characteristics	
Orbit	Sun-synchronous (descending local time: 10:30) Altitude 798km, Inclination 98.6deg
Mission Life	5 years
Scan	Push-broom electric scan (VNR) Wisk-broom mechanical scan (IRS)
Scan width	1150km cross track (VNR: VN & PL) 1400km cross track (IRS: SW & T)
Polarization	3 polarization angles for PL
Along track direction	Nadir for VN, SW and T, +45 deg and -45 deg for PL

					SNR at Lstd	IFOV
CH	λ	$\Delta\lambda$	L_{std}	L_{max}	VN, P, SW: SNR	
	VN, P, SW: nm T: μm		VN, P: W/m²/sr/μm T: Kelvin		T: NEΔT	m
VN1	380	10	60	210	250	250
VN2	412	10	75	250	400	250
VN3	443	10	64	400	300	250
VN4	490	10	53	120	400	250
VN5	530	20	41	350	250	250
VN6	565	20	33	90	400	250
VN7	673.5	20	23	62	400	250
VN8	673.5	20	25	210	250	250
VN9	763	12	40	350	1200	250/1000
VN10	868.5	20	8	30	400	250
VN11	868.5	20	30	300	200	250
P1	673.5	20	25	250	250	1000
P2	868.5	20	30	300	250	1000
SW1	1050	20	57	248	500	1000
SW2	1380	20	8	103	150	1000
SW3	1630	200	3	50	57	250
SW4	2210	50	1.9	20	211	1000
T1	10.8	0.7	300	340	0.2	250/1000
T2	12.0	0.7	300	340	0.2	250/1000
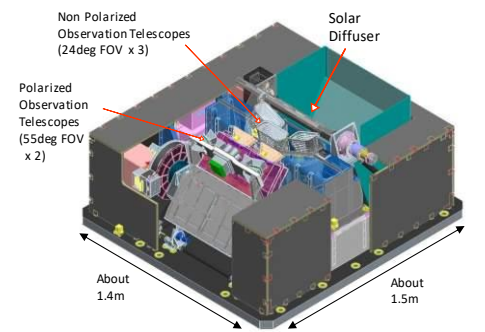
Visible and Near Infrared Radiometer (SGLI-VNR)
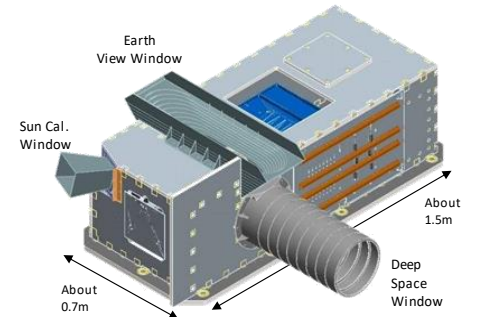
Infrared Scanning Radiometer (SGLI-IRS)

Figure 1. SGLI characteristics and overview of two radiometer units

performances obtained by the pre-launch characterization tests [5][6].

Figure 3 shows the radiometric gain trend of the reflective solar bands from the pre-launch characterization. The launch shift was evaluated by using the internal lamp data and in-orbit gain trend was obtained from the monthly lunar calibration data. The gain trend shows a slight declining tendency especially for the VNR shorter wavelength bands, but we conclude that all the SGLI bands keep within the 5 % absolute accuracy limit.

Calibration methodology	VNR	SWIR	TIR
Onboard calibrator			
Solar diffuser	Weekly	Weekly	-
Internal lamp	Weekly	Weekly	-
Blackbody	-	-	Every scan
Deep space	-	Every scan	
Dark image	Weekly	Weekly	-
Calibration maneuver			
Lunar calibration maneuver	Monthly		
Solar angle correction maneuver	Yearly		-
90-deg. yaw maneuver	Yearly	-	-
Vicarious calibration	Continued activities		
Cross calibration			
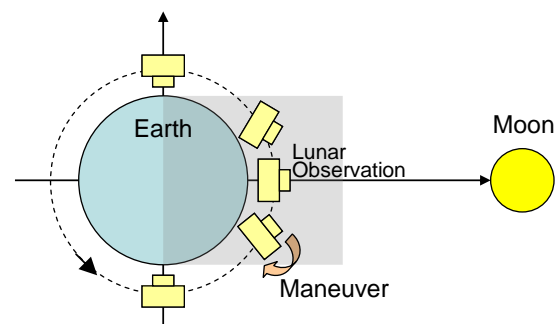
Figure 2. SGLI In-orbit calibration methodology and schematic view of the lunar calibration maneuver
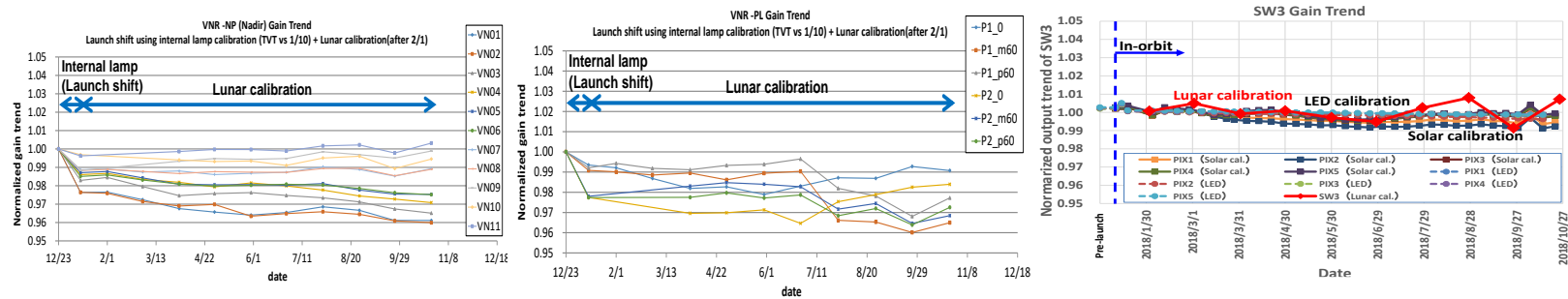
Figure 3. SGLI radiometric gain trend through one-year in-orbit operation

After the completion of the initial calibration and validation activities, JAXA publicly released the GCOM-C/SGLI products in December 2018 from the JAXA data distribution website (G-Portal: https://gportal.jaxa.jp/). All users can access all the standard products in open-free basis including the level 1 product (calibrated radiance product) and the 28 types of higher level products (geophysical variables) of Land, Atmosphere, Ocean and Cryosphere.[7][8].

JAXA expects that GCOM-C/SGLI products will contribute not only to climate change research but also to many fields of application including weather, fisheries, agriculture, disaster prevention (volcano, wild fire) and so on.

ACKNOWLEDGEMENT

REFERENCES

[1] Imaoka, K., Kachi, M., Fujii, H., Murakami, H., Hori, M., Ono, A., Igarashi, T., Nakagawa, K., Oki, T., Honda, Y., and Shimoda, H., "Global Change Observation Mission (GCOM) for Monitoring Carbon, Water Cycles, and Climate Change," Proc. IEEE Vol. 98 Issue 5 (2010)

[2] Okamura, Y., Tanaka, K., Amano, T., Shiratama, K., and Hosokawa, T., "Development and pre-launch test status of Second Generation Global Imager (SGLI)," Proc. SPIE 9639, 786209 (2015)

[3] Tanaka, K., Okamura, Y., Amano, T., Hiramatsu M., and Shiratama, K., "Operation concept of the second-generation global imager (SGLI)" Proc. SPIE 7862, 96390I (2010)

[4] Okamura, Y., Hashiguchi, T., Urabe T., Tanaka K., Yoshida J., Sakashita T. and Amano, T. "Pre-launch characterization and in-orbit calibration of GCOM-C/SGLI," Proc. IGARSS (2018)

[5] Tanaka, K., Okamura, Y., Mokuno M., Amano, Yoshida J., "First year on-orbit calibration activities of SGLI on GCOM-C satellite," Proc. SPIE 10781, 107810Q (2018)

[6] Urabe, T., Okamura, Y., Tanaka, K., Mokuno M., "In-orbit commissioning activities results of GCOM-C /SGLI," Proc. SPIE 10785, 107850N (2018)

[7] "GCOM-C "SHIKISAI" Data Users Handbook", link

[8]https://suzaku.eorc.jaxa.jp/GCOM_C/data/product_std.html

Discuss the Article

PROBA-V Yaw-maneuver results

By Stefan Adriaensen, Iskander Benhadj and Sindy Sterckx (VITO)

Currently, for more than five years in orbit, PROBA-V operations have been conducted successfully. The main focus of this small-satellite mission is the daily global monitoring of vegetation. This focus has led to many applications, including food-security and crop monitoring. Due to its operational autonomy, the platform is very agile and the command and control of acquisitions can be conducted in a flexible way. This ability is used, for instance, for the monthly lunar calibration acquisitions; the flexibility in the operations has already resulted in several extra-mission specific acquisitions, like the full coverage of Antarctica during wintertime.
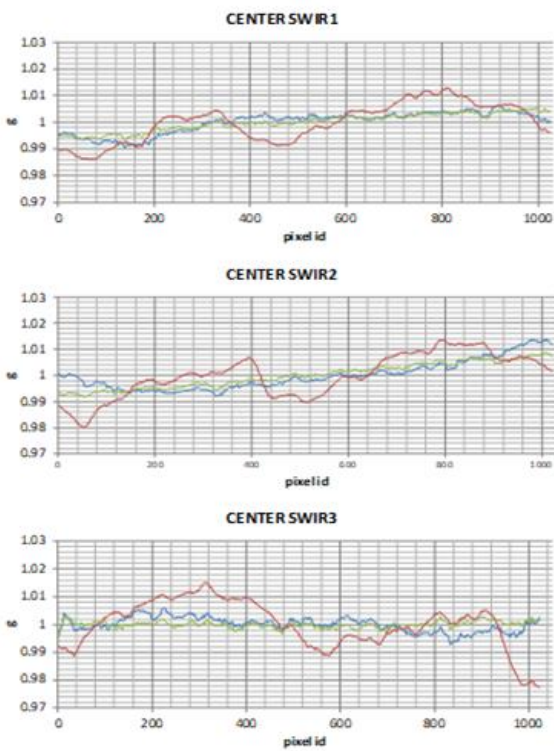
Figure 1: Results for the CENTER camera.
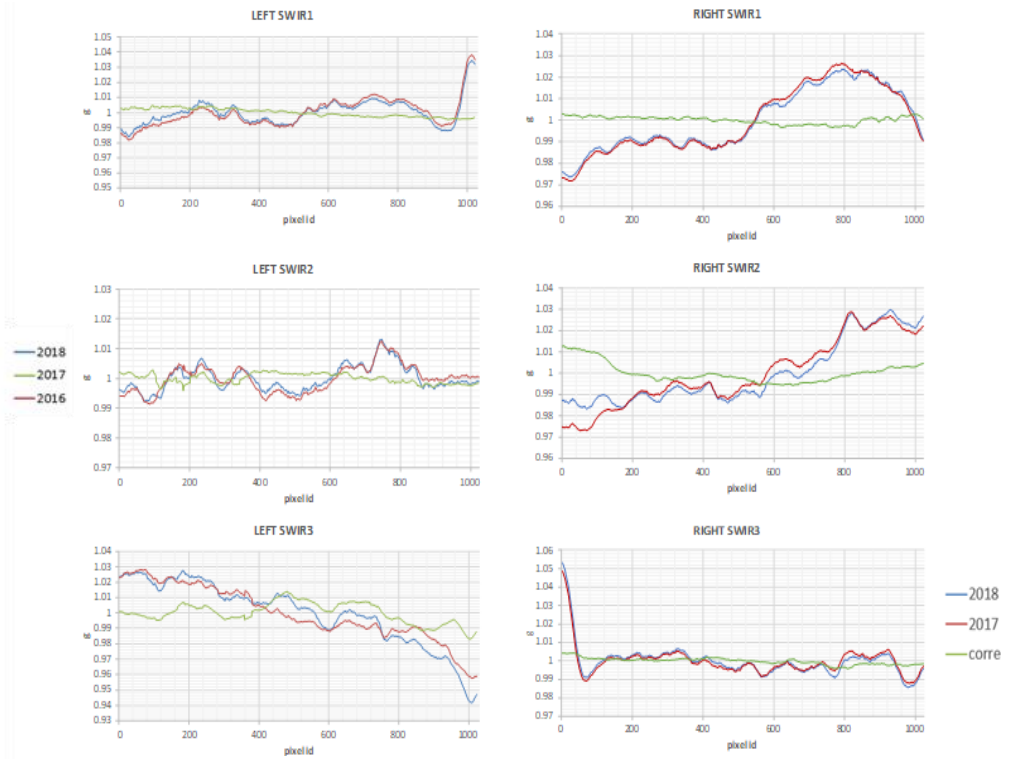
Figure 2: Results for LEFT and RIGHT cameras.

Due to the absence of on-board calibration devices, the radiometric calibration of the PROBA-V VNIR/SWIR optical instrument relies solely on vicarious calibration methods such as Lunar, Rayleigh and calibration over stable deserts and Deep Convective Clouds (Sterckx et al., 2016).

After the launch of the satellite, a significant remaining vignetting-effect was observed for the nine SWIR detectors (or strips). During commissioning, a correction method based on nominal acquisitions over radiometrically stable sites (e.g., Libya-4 PICS) was implemented and corrected the vignetting effects for a large part. However, due to its large swath on-ground, it was not possible to achieve a fully-fledged correction for all strips and still some remaining, low frequency, non-uniformities, were

observed but an exact quantification to allow for a proper correction remained difficult due to the absence of an on-board diffuser. A possible solution to this problem is known as a side-slither or 90° yaw-maneuver (Pesta F. at al, 015), to align FOV pixels into the flight-direction. Exactly the same position on ground is then recorded by all detectors of the same detector strip, allowing the assessment of relative detector to detector response variations.

PROBA-V has a rather complex design to cover the wide across-track angular view of 102°. The instrument is a combination of three identical camera's aligned across track. In nominal operation, the CENTER camera is pointed towards nadir, while both side-cameras (LEFT and RIGHT) are tilted 34° off-nadir, both in opposite direction. Every camera has two focal planes, one for the 3 VNIR spectral

bands and one for the SWIR band. The SWIR spectral band is a combination of three mechanically staggered detector strips, to cover the full swath. In total, 9 SWIR strips with 1024 detectors need to be considered for calibration of the Pixel Response Non Uniformity (PRNU). The VNIR strips are not considered, as they have no significant non-uniformity issues.

In March 2016 the first yaw-maneuver campaign was executed over the Niger-1 desert zone. During the summer of 2017 and 2018, follow-on campaigns were executed over the same radiometrically uniform desert site.

Method

The first yaw-maneuver calibration campaign was programmed on 11th March 2016. The acquired level 0 data (DN) for all SWIR strips is processed

by the PROBA-V Processing Facility up to un-projected level 1C Top Of Atmosphere reflectance, including the pixel-based geo-coordinate annotation. Within the uniform Niger-1 zone, a sub-zone is selected for every SWIR strip. The sub-zone is selected in such way that it allows multiple pixel selections per detector, located within this zone. Based on their geo-location, the un-projected pixels are selected from the image and sorted per detector. After averaging all pixels per detector, a low-pass filter removes the high frequency components form the intermediate PRNU profile. The remaining low frequency profile is then normalized to the mean value of all detector mean reflectance values. This normalized profile is the final profile, used to correct the existing PRNU calibration parameters. To gain confidence on the uniformity of the selected Niger-1 sub-zone, the zone itself is split-up in three separate mini-zones. For these mini-zones, again the same image processing procedure is applied. If all resulting mini-zone profiles are identical to the originally derived sub-zone profile, uniformity of the used zone is considered true. After applying this procedure for all nine strips, it was concluded that the correction is impossible for both off-nadir viewing cameras, with this type of yaw maneuver.

Therefore, in 2017 the yaw campaign was extended with two extra maneuvers for both side cameras. Each time one of the side cameras is pointed towards nadir viewing. This was achieved by two successive angular movements of the platform – a 90° yaw combined with approx. 10° roll maneuver (the magnitude of the roll is limited by star-tracker blinding avoidance). To calibrate all three cameras, three maneuvers have been

Table 1: Peak to peak pixel variation per strip and per camera before and after correction

%	LEFT		CENTER		RIGHT	
	before	after	before	after	before	after
SWIR1	5.0547	0.9261	2.6676	1.2539	5.4586	0.6167
SWIR2	2.0814	0.6754	3.3440	1.6354	5.5611	1.8621
SWIR3	8.5838	3.0782	3.7697	0.8014	6.0659	0.8676

performed in July and October 2017. In July 2018, follow-on maneuvers are executed, again separately for all three cameras.

Results

For the CENTER camera, results are presented in Figure 1. The red curve is the characterization of the PRNU (excluding the high frequency component), assessed with the 2016 yaw maneuver. Significant variations can be observed for all three cameras. The results are applied to correct the existing PRNU coefficients in the PROBA-V Radiometric Instrument Calibration files and applied in the nominal processing. The green (2017) and blue (2018) curves are the new yaw results, computed with the nominal parameters. Figure 2 shows the variation over the SWIR detectors for both left and right cameras for 2017 and 2018 yaw steering data. One can observe quite good agreement between both acquisitions for all strips. The green curve is after the application of the derived parameters of 2017 applied to the 2018 yaw results. The effective reduction in peak to peak variations is tabulated per strip in. More than 5% reduction can be observed for LEFT and RIGHT SWIR3 strips. LEFT SWIR1, CENTER SWIR3 and RIGHT SWIR3 clearly have remains of vignetting at the edges of the strips. After correction these effects are removed. Local features are reduced, resulting in increased flatting of the

PRNU profiles.

Conclusion:

Calibration of a wide swath instrument like PROBA-V has some challenges. Especially the specific design of the instrument and the absence of on-board radiometric calibrators forces the use of different vicarious calibration methods. Combined with the agility of the PROBA-V platform, the yaw maneuver correction is successfully applied. A simple pixel selection and correction algorithm has been developed. Inter-pixel non-uniformity has been reduced for all SWIR strips and all PRU profiles are significantly flattened. Relative improvements over 5% are achieved, reducing the detector variations to under 2% in all cases, except LEFT SWIR3. Follow-on maneuvers confirm the validity of the applied corrections.

References:

Sterckx, S., Adriaensen, A., Dierckx, W. and Bouvet M. (2016). In-Orbit Radiometric Calibration and Stability Monitoring of the PROBA-V Instrument. Remote Sensing, Vol. 8:7.

Pesta F., Bhatta S., Helder D. and Mishra N., Radiometric Non-*Uniformity* Characterization and Correction of Landsat 8 OLI Using Earth Imagery-Based Techniques. Remote Sensing, 2015, 7, 430-446.

NEWS IN THIS QUARTER

GOES-17 is GOES-WEST Now!

By Xiangqian "Fred" Wu and Fangfang Yu

On February 12, 2019, GOES-17 officially became GOES-WEST at 137.2°W, replacing GOES-15 in NOAA's operational satellite constellation. This event also marked the completion of upgrading NOAA with the new generation of advanced geostationary meteorological satellite. During the post-launch test of the GOES-17 Advanced Baseline Imager (ABI), a Loop Heat Pipe (LHP) anomaly was discovered that partially compromised its cooling capability. This anomaly leads to degraded data quality for some of the infrared channels during some hours at night on some days of the year. Despite these adversaries, great progress has been made to optimize the GOES-17 ABI performance and to improve its data quality, which enabled GOES-17 to join GOES-16 as a provider of visible and infrared imagery with high spatial, temporal, spectral, radiometric, and geometric quality in the Western Hemisphere.
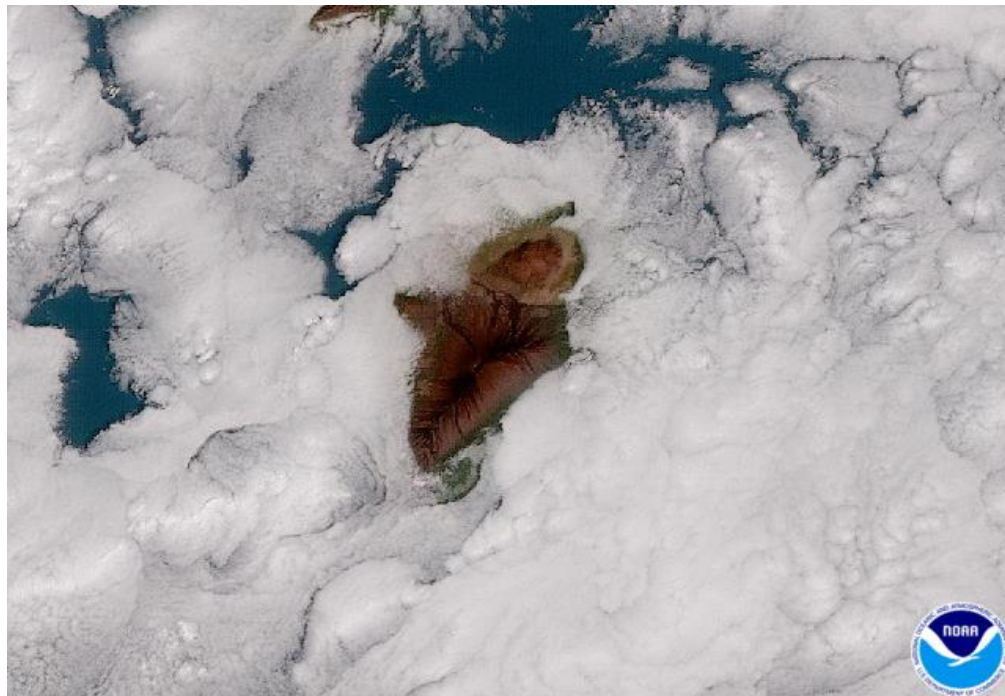
A GOES-17ABI color image of clouds around Hawaii's Big Island on Jan. 15, 2019 (https://www.nesdis.noaa.gov/content/goes-17-now-operational-here%E2%80%99s-what-it-means-weather-forecasts-western-us)

The figure above is an example of GOES-17 ABI color image over Hawaii's Big Island.

Discuss the Article

GSICS Session at Ninth Session of Asia Oceania Meteorological Users Conference (AOMSUC-9), Indonesia

By Mitch Goldberg (GSICS EP Chair) and Mr. Andersen Panjaitan (BMKG)

The Ninth Asia/Oceania Meteorological Satellite Users' Conference (AOMSUC-9) was held in Bogor and Jakarta, Indonesia from 6-11 October 2018. It was hosted by the Indonesian Agency for Meteorology, Climatology and Geophysics (BMKG). Indonesia. Among range of topics (e.g., Training, Nowcasting, and Earth Observations) the meeting also held a GSICS Session. The GSICS Session was co-chaired by Dr. Mitch Goldberg (GSICS EP Chair,

NOAA) and Mr. Andersen Panjaitan (BMKG). There were four oral presentations in the GSICS session and a related poster presentation. The first presentation was given by Mr, Yusuke Yogo of JMA on the Himawari-8, -9 / AHI Radiometric Calibration and Validation using GSICS: Their Importance and Benefits. JMA operates two meteorological satellites, Himawari-8 and 9, and implements the Cal/Val methods discussed in GSICS to

their observation data operationally. The presentation discussed the importance of satellite radiometric calibration for users and the outline of Cal/Val methods implemented by JMA and other GSICS members, particularly a method of comparing between observations and calculated values derived from a radiative transfer model.

Participants in the AOMSUC -9

The second talk, by Dr. Alexander Uspensky of Roshydroment, provided a comprehensive description of the on Cal/Val plan developed by SRC "Planeta" (Roshydromet). The SRC "Planeta" contributes to GSICS as a Processing and Research Center for Russian Meteorological Satellites including polar-orbiting "Meteor-M" series and geostationary "Electro-L" series. It aims to provide users with consistent well-calibrated measurements from operational Meteor-M and Electro-L satellites as well as the results of satellite-based products validation. The Cal/Val website of SRC "Planeta" is divided into three sections. The first section, called "Calibration-intercalibration issues" provides information on the on-board calibration monitoring and post-launch calibration (inter-calibration) products (**http://planet.rssi.ru/calval/calibration-en**) for basic instruments of both polar-orbiting Meteor-M satellites and geostationary Electro-L satellites. This applies to the imaging/sounding instruments of current and future "Meteor-M" satellites (VIS, NEAR-IR and IR channels of MSU-MR, Infrared Fourier Spectrometer IKFS-2, Microwave Imaging Sounding Radiometer MTVZA-GY, Onboard Radar Complex BRLK) and imaging

instrument of Electro-L satellites (VIS and IR channels of MSU-GS). The second section of the website "Validation" contains the validation results for the products derived from measurements of "Meteor-M" and "Electro-L" instruments listed above. The validation is being performed for the following products: cloud cover and precipitation parameters, sea surface temperature, vertical profiles of atmospheric temperature and humidity, wind vectors, sea level wind, total ozone in the atmosphere, total content of carbon dioxide and methane in the atmosphere, snow cover parameters, boundaries of the Arctic sea ice cover distribution. The third section of the website is the Data Archives that contains files of "Meteor-M" and "Electro-L" basic instrument measurements together with measurements of some foreign satellites collected for several pre-selected test polygons.

The third talk was given by Dr. Xiuqing (Scott) Hu (Chair, GSICS Research Working Group) of CMA on the use of GSICS to evaluate FY3D, which was launched on November 15, 2017 in the 1400 afternoon orbit. The key performance evaluation of FY-3D MERSI-II and HIRAS including the spectral calibration, radiometric

calibration and geolocation accuracy was conducted by using CMA's GSICS platform. The GSICS-consensus reference instruments, IASI, CrIS, MODIS and VIIRS, are used to evaluate the radiometric accuracy of MERSI-II and HIRAS. In addition to this, the accurate collocation and inter-comparison between MERSI-II and HIRAS at the same satellite platform gave us several important information of their performance, especially the knowledge of HIRAS subpixel geolocation shift. Based on the above GSICS evaluation, mechanism behind radiometric calibration bias of MERSI-II and HIRAS also were found including the non-linearity, polarization effect and other parameters of the instruments. These parameters were updated several times based on comprehensive assessment and iterative validation during the commissioning test.

The fourth and final presentation in this session was given by Dr. Chunqiang Wu of CMA on the detail commission of the High-Spectral Infrared Atmospheric Sounder (HIRAS) instrument. The HIRAS is a space-borne Fourier transform spectrometer (FTS) onboard the Polar-orbiting FengYun 3D (FY-3D) satellite and is the first CMA hyperspectral infrared

sounder in polar orbit. HIRAS provides measurements of Earth view interferograms in three infrared spectral bands at 29 cross-track positions, each with a 2 × 2 array of field of views (FOVs). The HIRAS ground processing software transforms the measured interferograms into calibrated and navigated spectra in the form of Sensor Data Records (SDRs) that cover spectral bands from 650 to 1140 cm-1 (Longwave Band, LW), 1210 to 1750 cm-1 (Midwave Band, MW), and 2155 to 2550 cm-1 (Shortwave Band, SW) with spectral resolutions of 0.625 cm-1, 1.25cm-1, and 2.5 cm-1, respectively. During the time of the intensive calibration and validation (ICV) period from 1 March to 31 July of 2018, the HIRAS performance, including noise, spectral frequency accuracy and

radiometric uncertainty were characterized under the framework of Global Space-based Inter-Calibration System (GSICS) and the requirements of the Numerical Weather Prediction (NWP) systems. The Noise Equivalent Differential Radiance (NEdN) is estimated from the cold space, internal calibration target (ICT) and Earth view measurements. It was separated into correlated noise and un-correlated noise. To reduce the correlated noise to well below the uncorrelated noise level, the alignment of the interferometer's stationary mirror was adjusted. As a result of the adjustment, the total NEdN values have met the specifications except for a narrow spectral region at the left end of LW band. In spectral frequency calibration, the effects of the beam divergence are corrected by the

inverse of the self apodization matrices with the instrument line shape (ILS) parameters derived by using both ground thermal vacuum (TVAC) and on-orbit measurements by minimizing the spectral difference between the measurements and Line-BY-Line (LBL) radiative transfer model (RTM) calculations.

In addition to the talks, a poster made under this session topic by Xueyan Hou of CMA entitled "Calibration of FengYun-3D Microwave Humidity Sounder using GPS Radio Occultation Data" was particularly interesting for the GSICS community. Presentations can be downloaded from http://aomsuc9.bmkg.go.id/presentations/

Reference:

AOMSUC-9 Summary Report: http://aomsuc9.bmkg.go.id/summary/

[Discuss the Article]

Announcements

ESA and SITP join GSICS Team

By Lawrence E. Flynn (Director GSICS Coordination Center)

The European Space Agency (ESA) and the Shanghai Institute for Technical Physics (SITP) were formally admitted as GSICS Members. The announcement was made by Dr. Mitch Goldberg (GSICS EP Chair) in the recently held GSICS Annual Meeting in Frascati, Italy.

In recent years, ESA (www.esa.int) has had an observer status on the GSICS EP. Formed by the EU member space agencies, ESA has contributed immensely to WMO/CGMS goals of Earth observation missions using collaborative cooperation among space

agencies. This has continued with its recent launches of the Copernicus Earth Observation missions.

The SITP is an independent Chinese Academy of Science (CAS) Institute. SITP's primary research area is the application of infrared physics and optoelectronics technology with particular attention to new infrared photoelectric materials, devices and methods. SITP focuses on developing advanced airborne and space-borne payloads, infrared staring imaging and signal processing, infrared focal plane arrays and infrared photoelectric

devices, optical coatings, miniature coolers, medical image processing and remote sensing information processing. The institute comprises 14 research departments, a national key laboratory for infrared physics, a national key laboratory for sensors (the photo-sensor branch) and three CAS key laboratories.

On behalf of GSICS, we welcome ESA and SITP, and look forward to their sustained and continued contributions in shaping the future of GSICS.

FIDUCEO Workshop - New Climate Data from Space: Exploitation for Science and Services. Lisbon 25-27 June, 2019.

By Chris Merchant, University of Reading

The FIDUCEO team announces its second workshop exploring the application of metrological concepts to the domain of Earth Observation and climate, following on from the first workshop last year. The focus of the second workshop is developing and exploiting Climate Data Records (CDRs) with evaluated uncertainties. This theme addresses the following: the link between uncertainty in Fundamental Climate Data Records (FCDRs) and derived CDRs; providing and exploiting uncertainty information for CDRs; and sharing experiences on these topics from within and beyond the FIDUCEO project.

The whole programme starts with a training session on Metrology for EO on the morning of Tuesday 25th June.

- Training session: Concepts of Metrology for Earth Observation; metrological methods and their application in the EO domain, including principles and exercises

The FIDUCEO workshop sessions commence Tuesday afternoon and continue to Thursday lunchtime:

- Session 1: Fundamental Climate Data Records principles and methods: Sharing practice in producing FCDRs. FCDR producers/ designers are invited to present their experience and approaches
- Session 2: Deriving Climate Data Records (CDRs) from FCDRs. Sharing practice on deriving CDRs and the links between FCDR and CDR properties, including uncertainties and FIDUCEO concepts for uncertainty propagation. CDR producers/ designers are invited to present their experience and approaches
- Session 3: Long term stability of Fundamental Climate Data Records and Climate Data Records: Methods and implementation; Intercalibration,

harmonisation, CDR ensembles, fiducial references. FCDR/CDR producers/ designers are invited to present their experience and approaches

- Session 4: Application of new methods to climate/environmental data record creation in a FIDUCIAL world, FIDUCEO lessons learned and user recommendations. Discussion panel including feedback from poster sessions.

We warmly welcome abstracts for presentations for the relevant sessions. The committee will select submissions for poster or oral presentation to ensure a good balance of material in plenary sessions and lively poster viewing. Details regarding **Registration, Abstract Submission and Deadlines** can be obtained via **http://www.fiduceo.eu/content/2nd-fiduceo-workshop-0**

CEOS, GSICS Workshop: An SI Traceable Space–based Climate Observing System, London UK, September 9-11, 2019

By Nigel Fox (NPL)

Recent years have seen an increasing urgency from international coordinating bodies such as CEOS, WMO, GSICS, GCOS, climate researchers, and policy makers to establish *a space-based climate observing system* capable of unambiguously monitoring indicators of change in the Earth's climate, as needed for international mitigation strategies such as the 2015 Paris climate accord. Such an observing system

requires the combined and coordinated efforts of the world's space agencies. To deliver data that can be considered unequivocal on decadal timescales, facilitating policy makers to make decisions in a timely manner, requires improvements to heritage, existing, and in-development space assets. In particular, observations spanning the electromagnetic spectrum from the near-UV to microwave need to be of sufficient accuracy and

duration, traceable to the International System of Units (SI), and sampled to ensure global representation in order to detect change in as short a timescale as possible. The harshness of launch and the space environment has to date limited any satellite mission's ability to robustly demonstrate SI traceability on-orbit at the accuracy and confidence levels needed. *An order of magnitude improvement is typically required for robust*

climate observations.

Although not as demanding in terms of long-term accuracies, implementing such a system also facilitates improvements to *operational applications*, particularly where data harmonisation enables 'information on-demand' for a wider range of applications such as health, a sustainable food supply, and pollution.

Bringing together experts from space agencies, industry, academia, and policy makers, the intent of this international workshop is a community strategy to quantify the *benefits and consequential specifications of a space-based climate observing system* along with a roadmap to implementation.

Discussion topics include:
- Potential scientific and economic benefits
- The state-of-the-art in establishing traceability in orbit: current technologies, methods, and missions (e.g.

CLARREO and its Pathfinder, TRUTHS, and Chinese and Indian counterparts).
- New observation and climate-sensitivity detection capabilities and concepts

Stimulated by invited and contributed presentations, the workshop will be structured to ensure ample discussions on all topics. An introductory session will be suitable for a broad audience. This will be followed by more detailed technical discussions, and conclude with a final session focusing on defining observing-system requirements and a draft implementation strategy. The latter will require pre-workshop preparations.

Formal contributions are solicited related to the following themes, which form the basis of **sessions in the workshop**:

Science and societal drivers for the climate and operational communities (including economic benefits) Observations and datasets needed (measurements, timescales, and accuracies) Reference calibrations (facilities/targets, approaches, capabilities, and uncertainties) Mission/technologies/concepts under development or conceived (status, technical capabilities) Develop community 'white paper' on benefits, needs, and a proposed implementation architecture.

Pre-registration for this open workshop is required for the venue.

Please submit a *300- to 500-word abstract* by April 10, 2019 to events@npl.co.uk stating clearly how it addresses the scope and themes of the workshop. The meeting webpage is available at **https://www.eventbrite.co.uk/e/ceos-wmo-gsics-workshop-registration-55697497715**

GSICS-Related Publications

Berg, Wesley, Rachael Kroodsma, Christian D. Kummerow, and Darren S. McKague. 2018. 'Fundamental Climate Data Records of Microwave Brightness Temperatures'. *Remote Sensing* 10 (8): 1306. doi:10.3390/rs10081306.

Ebrahimi, Hamideh, Saswati Datta, and W. Linwood Jones. 2018. 'Intercalibration of Cross-Track Scanners in GPM Constellation'. *Ieee Transactions on Geoscience and Remote Sensing* 56 (10): 5749–57.doi: 10.1109/TGRS.2018.2825333

Okuyama, A., M. Takahashi, K. Date, K. Hosaka, H. Murata, T. Tabata, and R. Yoshino. 2018. 'Validation of Himawari-8/Ahi Radiometric Calibration Based on Two Years of in-Orbit Data'. *Journal of the Meteorological Society of Japan* 96B: 91. doi: 10.2151/jmsj.2018-033.

Rublev, A.N., E.V. Gorbarenko, V.V. Golomolzin, E.Y. Borisov, J.V. Kiseleva, Y.M. Gektin, and A.A. Zaitsev. 2018. 'Inter-Calibration of Infrared Channels of Geostationary Meteorological Satellite Imagers'. *Frontiers in Environmental Science* 6 (NOV). doi: 10.3389/fenvs.2018.00142.

Wang, L., X. Hu, L. Chen, and L. He. 2018. 'Consistent Calibration of VIRR Reflective Solar Channels Onboard FY-3A, FY-3B, and FY-3C Using a Multisite Calibration Method'. *Remote Sensing* 10 (9).doi: 10.3390/rs10091336.

Wu, Wan, Xu Liu, Xiaoxiong Xiong, Yonghong Li, Qiguang Yang, Aisheng Wu, Susan Kizer, and Changyong Cao. 2018. 'An Accurate Method for Correcting Spectral Convolution Errors in Intercalibration of Broadband and Hyperspectral Sensors'. *Journal of Geophysical Research-Atmospheres* 123 (17): 9238–55. doi: 10.1029/2018JD028585.

Submitting Articles to the GSICS Quarterly Newsletter:

The GSICS Quarterly Press Crew is looking for short articles (800 to 900 words with one or two key, simple illustrations), especially related to calibration / validation capabilities and how they have been used to positively impact weather and climate products. Unsolicited articles may be submitted for consideration anytime, and if accepted, will be published in the next available newsletter issue after approval / editing. Please send articles to manik.bali@noaa.gov.

With Help from our friends:

The GSICS Quarterly Editor would like to thank Tim Hewison (EUMETSAT), Fangfang Yu (NOAA), Tony Reale (NOAA) and Lawrence E. Flynn (NOAA) for reviewing articles in this issue.